Tearing Mode Driven Charge Transport and Zonal Flow in the MST Reversed Field Pinch

W.X. Ding[1], D.L. Brower[1], D. Craig[2], B.H. Deng[1], G. Fiksel[2], V. Mirnov[2], S.C. Prager[2], J.S.Sarff[2], V.Svidzinski[2]

[1]University of California, Los Angeles, California   90095 USA
[2]University of Wisconsin-Madison, Madison, Wisconsin   53706 USA

e-mail contact of main author: wding@wisc.edu

Abstract: First direct measurements of non-ambipolar magnetic fluctuation-induced charge (or particle) transport and Maxwell stress in the interior of a high-temperature plasma are reported. These effects are driven by global resistive tearing modes and are measured in the vicinity of the resonant surface for the dominant core resonant mode by using a high-speed laser-based Faraday rotation diagnostic. Charge transport, observed in bursts at the sawtooth crash, results from an imbalance between the magnetic fluctuation-induced ion and electron radial particle fluxes and is locally non-ambipolar. Observation of significant charge flux originates from nonlinear multimode mode interactions and has two important implications. First, it generates a potential well along with locally strong electric field and electric field shear at the resonant surface. Second, this electric field results in a spontaneous $E \times B$ driven zonal flow.

1. Introduction

Flow in a plasma can arise from several causes. For instance, Maxwell or fluid Reynolds stresses from fluctuations can produce flow, as is the case for zonal flows driven by electrostatic turbulence in tokamaks [1,2]. Flows can also arise from radial electric fields (and resulting E x B drifts) that are produced by the differential (non-ambipolar) radial transport of ions and electrons. Non-ambipolar transport would be expected to occur in the presence of stochastic magnetic fields since electrons stream more rapidly along field lines. Stochastic magnetic fields can be driven by tearing instabilities [3,4,5], that often underlie the sawtooth oscillation, or by deliberate application of perturbing field (as in ergodic divertors). The relation between fluctuations, transport, electric field, and flow is an interesting one of many coupled processes.

Fluctuation-induced particle flux can generally be described by [6]

$$\Gamma_\alpha = \frac{\langle \delta n \delta E_\perp \rangle}{B} + \frac{\langle \delta j_{//,\alpha} \delta b_r \rangle}{q_\alpha B} ,$$ (1)

where the <…> denotes a flux surface averaged product of the fluctuation quantities (density δn, electric field $\delta E_\perp$, parallel current density $\delta j_{//,\alpha}$ ($\alpha = i,e$) or radial magnetic field δb_r fluctuations) and B is the equilibrium magnetic field. The two terms on the right hand side represent the electrostatic and electromagnetic fluctuation-induced particle fluxes, respectively. The magnetic term is intrinsically non-ambipolar due the dependence on species charge. Therefore, the difference between the fluctuation-induced ion and electron fluxes, referred to here as the charge flux, can be written as

$$\Gamma_q = \Gamma_i - \Gamma_e = \frac{< \delta j_{//} \delta b_r >}{eB} ,$$ (2)

where $\delta j_{//}$ is the current density fluctuation along the equilibrium magnetic field. The charge flux associated with magnetic stochasticity is identically given by the correlated product of parallel current density fluctuations and radial magnetic field fluctuations. Magnetic fluctuation-induced particle transport has been studied for many years (see [6] and references therein) but all previous measurements were made by insertable probes and consequently limited to the cooler edge region of hot plasmas. In the edge, it was found that particle losses induced by magnetic field fluctuations were ambipolar ($<\delta j_{//}\delta b_r>\approx 0$) resulting from a $\pi/2$ phase difference between parallel current density and radial magnetic fluctuations [7,8,9]. More recent measurements suggest this may no longer hold true, as probes are inserted deeper into the plasma [10], implying the presence of non-ambipolar magnetic fluctuation-induced particle transport. Theoretically, a non-ambipolar flux can be balanced by an opposing non-ambipolar flux to maintain plasma quasi-neutrality [11]. Furthermore, quasi-linear kinetic theory reveals that the charge flux is not pointwise zero for a localized normal mode and ambipolarity can still be realized on a spatial average [12].

In this paper, we explore experimentally the case where magnetic field lines become stochastic during the crash phase of a sawtooth oscillation in the reversed field pinch (RFP) configuration. We perform measurements from which one can infer the presence of a mean flow (toroidally and poloidally symmetric) that is strongly localized about the reconnection surface of the inner-most core resonant mode. Flows within a magnetic surface that are radially localized and symmetric are often called zonal flows. The key observations, made in the interior of the high-temperature MST (Madison Symmetric Torus) RFP, are achieved by direct measurement of the radial charge flux (i.e., the difference between ion and electron fluctuation-induced fluxes) arising from magnetic fluctuations. These fluctuations and their correlated product are measured using a non-perturbing high-speed laser-based Faraday rotation diagnostic. Charge flux is associated with the radial derivative of the Maxwell stress whose amplitude and spatial distribution are also resolved. Measurements, focusing on dominant core-resonant tearing mode (with poloidal and toroidal mode number, m,n=1,6) in MST plasmas, show that the Maxwell stress is large, peaking at the resonant surface. The radial charge flux from magnetic fluctuations alone is also measured to be localized to the mode-resonant surface and to be extremely large ($\sim$ 1% of the total radial particle flux). Origin of large magnetic fluctuation-induced charge flux is experimentally connected to nonlinear 3-wave coupling. The charge flux by itself would lead to a huge radial electric field during a sawtooth crash. However, the large time-dependent field generates a large and opposing radial polarization drift that nearly cancels the flux from magnetic fluctuations. The net result, *calculated* from the measured magnetically-induced flux (including the inferred polarization drift and viscous damping), is a charge separation that produces a large radial electric field and radial electric field shear. These fields act to generate a substantial and spontaneous E x B zonal flow at the resonant surface.

2. Experimental Measurement

Measurements reported herein were carried out on the MST RFP [13,14] whose major radius R_o=1.5 m, minor radius a=0.52 m, discharge current 350~400 kA, line-averaged electron density $\bar{n}_e \sim 1\times 10^{19}\ m^{-3}$, electron temperature $T_e \sim T_i \sim 300 eV$, and effective charge number Z_{eff}=2~6. Equilibrium and fluctuating magnetic fields are measured by a fast (Δt~4 μs) Faraday rotation diagnostic where 11-chords (chord separation ~8 cm) probe the plasma

cross section vertically [15]. MST discharges display a sawtooth cycle in many parameters and measured quantities are ensemble (flux-surface) averaged over these reproducible sawtooth events. All fluctuation measurements refer to the core resonant (m/n=1/6) mode (laboratory frame frequency ~ 15-20 kHz) whose resonant surface is located at r/a=0.35.

Before proceeding to describe the measurements, it is useful to first express Eq.(2) in a form most suitable for experimental determination. The flux surface averaged quantity can be rewritten as

$$< \delta j_{//} \delta b_r > = < \delta j_\phi \delta b_r > \frac{B_\phi}{B} + < \delta j_\theta \delta b_r > \frac{B_\theta}{B} \qquad , \qquad (3)$$

where ϕ, θ are the toroidal and poloidal directions, respectively. This equation can be further simplified by using Ampere's law $\nabla \times \delta B = \mu_0 \delta J$ and Gauss' law $\nabla \bullet \delta B = 0$ for a fluctuating mode, leading to

$$< \delta j_{//} \delta b_r > \approx \frac{1}{\mu_0} \frac{R}{nB} < \delta b_r \frac{\partial}{\partial r} \delta b_\theta > (\vec{k} \bullet \vec{B}) \qquad , \qquad (4)$$

where $\vec{k} \bullet \vec{B} = \frac{n}{R} B_\phi + \frac{m}{r} B_\theta (=0$ at resonant surface). An additional term, $\frac{B_\phi}{B}(1 - \frac{B_\theta R m}{B_\phi n r}) \frac{< \delta b_r \delta b_\theta >}{r}$, is not included in Eq.(4) as it is found to be small in the vicinity of the resonant surface, $|(r - r_s)/r_s| << 1$, where r_s is resonant surface location [15]. It is important to note that the term $< \delta b_r \partial \delta b_\theta / \partial r >$ in Eq.(4) is the dominant component of the Maxwell stress ($< \delta b_r \delta b_\theta >$) radial derivative for the region near the resonant surface where both δb_θ and $\partial \delta b_r / \partial r$ are small.

The radial derivative of δb_θ is directly obtained by measuring the current density fluctuations ($\delta j_\phi \approx 1/\mu_0 \partial \delta b_\theta / \partial r$) which generate the magnetic perturbation, as shown in Fig.1(a), through use of a novel polarimetry technique [15,16]. Current density fluctuations slowly increase during the linear phase of the sawtooth cycle and surge at the crash. The phase (δ) between current density and radial magnetic field fluctuations, shown in Fig.1(b), is nearly $\pi/2$ away from the sawtooth crash, making the cosine of phase near zero. This implies the magnetic fluctuation-induced particle transport is approximately ambipolar. However, when approaching the crash, the phase deviates from $\pi/2$ generating significant magnetic fluctuation-induced charge flux. This, in turn, results in non-ambipolar transport near the resonant surface. The charge flux spatial maxima over a sawtooth event is seen in Fig.1(c), and shows a peak of ~ 4×10^{19} $m^{-2} s^{-1}$ at the crash. This is equivalent to ~1% of the measured total radial particle flux [17]. At other times the charge flux is reduced to ~ 10^{18} $m^{-2} s^{-1}$.

The charge flux spatial profile is determined by the mode helicity, Maxwell stress radial derivative and equilibrium magnetic field distribution according to Eq.(4). Spatial profiles of magnetic field and current density fluctuations can be reconstructed from line-integrated fluctuation measurements as previously described [16] with the result shown in Fig. 2, for the dominant, core resonant ($m/n = 1/6$) mode just prior to the sawtooth crash. Radial magnetic

fluctuations broadly peak near the resonant surface and fall off rapidly toward the conducting wall. Finite δb_r inside the resonant surface indicates that reconnection is taking place. Poloidal magnetic fluctuations change sign across the resonant surface due to the localized perturbation current sheet. Current density fluctuations ($\delta j / J_0 \sim 4.5\%$) peak at the mode resonant surface with width ~8 cm, greater than linear MHD predictions.

The radial derivative of Maxwell stresses is determined by the measured spatial distribution of radial magnetic field and current density fluctuations plus their respective phase. The phase information between δj_ϕ and δb_r can be obtained by ensemble averaging. In MST, rotation of the low-n magnetic modes transfers their spatial structure in the plasma frame into a temporal evolution in the laboratory frame. Since the magnetic modes are global, for convenience we correlate δj_ϕ to a specific helical magnetic mode obtained from spatial Fourier decomposition of measurements from 64 wall-mounted magnetic coils. After averaging over an ensemble of similar events, we can directly determine the phase between $\delta j_\phi(r_s)$ and $\delta b_\theta(a)$ for the specified mode. Since (1) $\delta b_r(a)$ and $\delta b_\theta(a)$ have a fixed phase difference of $\pi/2$ at the edge where $j_r = 0$ and (2) the radial magnetic perturbation is expected to have a constant phase at all radii for tearing modes (which has been verified by probe measurements in lower temperature plasmas), we are able to determine the phase between $\delta j_\phi(r_s)$ and $\delta b_r(r_s)$. Using this information, along with the magnitude of $\delta b_r(r_s)$ from Fig. 2, we are able to evaluate $<\delta j_\phi(r_s)\delta b_r>$ to determine the radial derivative of Maxwell stress in the vicinity of the rational surface as shown in Fig. 3. This Maxwell stress derivative (equivalent to torque in the ion momentum equation) is localized near ($m/n=1/6$) mode resonant surface and has spatial extent comparable to the magnetic island width. Combining information on the Maxwell stress with the equilibrium field distribution [18] allows us to determine the spatial profile of charge flux at a sawtooth crash as seen in Fig. 4. Charge flux is zero at the resonant surface because the radial magnetic field is perpendicular to the equilibrium magnetic , i.e., $\vec{k} \bullet \vec{B} = 0$. However, on either side of the resonant surface the charge flux is non-zero and changes sign due to magnetic shear (i.e., $\vec{k} \bullet \vec{B}$ changes sign [see Eq.(4)]). Details of the profile structure and amplitude are subject to rather large error bars due to limitations related to measurement spatial resolution and numerical inversion errors.

The existence of non-vanishing charge flux in MST plasmas most likely originates from nonlinear interactions between multiple modes since magnetic fluctuations can interact with the eddy currents generated by global magnetic field perturbations. This is similar to the effect of an error field or imposed boundary [19]. Experimentally, observed changes in fluctuation amplitude [Fig. 1(a)] and phase [Fig. 1(c)] during a sawtooth crash act to enhance the charge flux. In MST RFP, resonant low-n (n=6 is the resonant mode closest to the magnetic axis), m=1 magnetic modes dominate the core magnetic fluctuation wave number spectrum. In addition to the core resonant modes, m=0 (n=1, 2,..) modes are resonant at the reversal surface where toroidal magnetic field goes to zero (near plasma edge). Both the m=1 and m=0 tearing modes have a global nature so that nonlinear mode coupling is common [20,21,22]. The 3-wave interaction has to satisfy the sum rule $m_1 \pm m_2 = m_3$ and $n_1 \pm n_2 = n_3$. Coupling of two adjacent m=1 modes via interaction with an m=0 mode has been shown to be very important in both experiments and MHD computation.
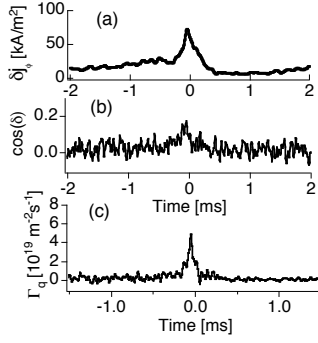
Fig. 1. (a) Current fluctuations ; (b) phase between current and magnetic field fluctuation for m/n=1/6 mode; (c) the charge flux. The t=0 denotes sawtooth crash.
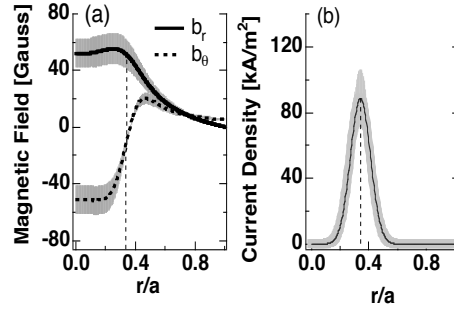

Fig. 2. (a) Magnetic field and (b) current density fluctuation spatial profile for *m/n=1/6* mode. Mode resonant surface is at r/a=0.35. The shaded region indicates measurement uncertainty.
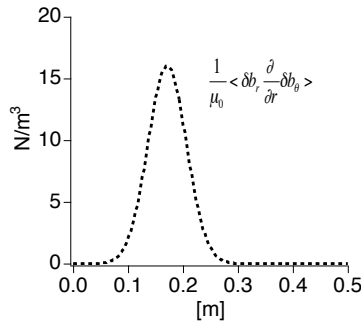

Fig. 3. Spatial profile of radial derivative of Maxwell stresses. This force peaks at resonant surface with a finite width about 8 cm.
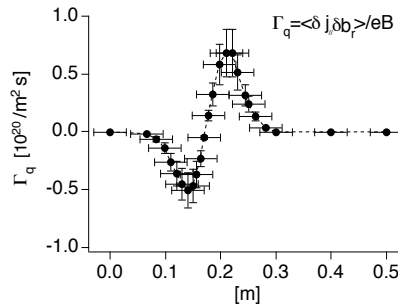

Fig. 4. Magnetic fluctuation-induced charge flux (difference between electron flux and ion flux) spatial distribution. Flux changes sign across resonant surface at r=0.17m .
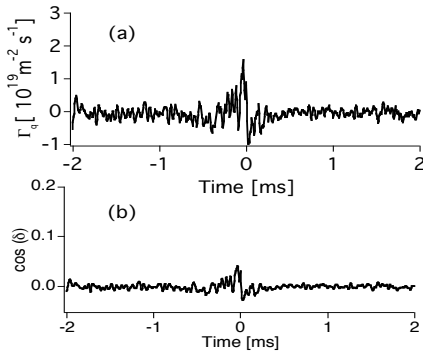

Fig. 5. (a) Magnetic induced charge flux dynamics over sawtooth for plasmas where m=0 mode is removed; (b)Phase between current fluctuations and radial magnetic fluctuations where m=0 mode is removed.

A typical strong three wave interaction observed in MST plasmas is that between the (1,6), (1,7) and (0,1) modes. Consequently, by suppressing one of the interacting modes, we expect a reduction in the nonlinear mode coupling. In order to identify the role played by nonlinear coupling in the charge flux during the sawtooth crash, we compare standard RFP plasmas with those where the reversal surface has been removed (i.e., non-reversed MST plasmas where the reversal surface for the m=0 mode is located at $r \geq a$, i.e., at or beyond the plasma boundary). For non-reversed plasmas, the m=1 mode amplitude ($\delta b_\theta(a)$) during the sawtooth cycle remains comparable to the reversed case. However, the m=0 mode amplitude is significantly reduced since its resonant surface is removed. For non-reversed plasmas, measurements reveal the charge flux is similarly reduced, up to 5-fold, compared to standard

RFP plasmas as shown in Fig. 5(a). This occurs primarily because the phase difference between localized current density fluctuations and global radial magnetic field fluctuation for the (1,6) mode is also altered, deviating only slightly from π/2, as shown in Fig. 5(b). From these results it clear that significant phase deviation from π/2 requires substantial m=0 activity. This implies the phase change between δj_ϕ and δb_r for the (1,6) mode occurs largely due to nonlinear coupling.

3. Radial Electric Field Generation and Zonal Flow

A non-vanishing charge flux, shown in Fig. 4, indicates that the magnetic fluctuation-induced particle transport is non-ambipolar, at least locally. As a consequence, plasma quasi-neutrality implies that large radial electric fields will quickly appear. To gain insight into the potential implications of magnetic fluctuation-induced charge flux on plasma dynamics, we use the quasi-linear kinetic equation [12] for perpendicular momentum balance to evaluate the fluctuating radial electric field according to

$$\varepsilon_0 \varepsilon_\perp \frac{\partial E_r}{\partial t} = -\frac{<\tilde{j}_{//}\tilde{b}_r>}{B} - \frac{\mu}{B}\nabla^2 V_{E\times B} \quad , \qquad (5)$$

where the first term on the right hand side is particle flow generated by magnetic fluctuations and the second term describes classical viscous forces with viscosity coefficient μ. Fast temporal variations in electric field will generate an ion polarization drift to offset the effect of electrons streaming along stochastic field lines [23]. This effect is included by use of the perpendicular dielectic constant, $\varepsilon_\perp = 1 + c^2/V_A^2$, (where V_A is Aflven speed) which is of order 10^4 for MST plasmas. Lastly, $V_{E\times B} = -E_r/B$ is fluctuation-induced mean flow. Other terms [24] in Eq.(5) are either estimated to be smaller than $<\tilde{j}_{//}\tilde{b}_r>/B$ for MST plasmas or are ignored. Numerical integration of Eq.(5) can be performed to solve for the radial electrical field evolution using boundary conditions $E_r(r=0,a)=0$, where $<\tilde{j}_{//}\tilde{b}_r>/B$ is the measured magnetic-induced charge flux. The classical perpendicular viscosity $v^* = \mu/\rho$ ($\sim nkT_i/\omega^2_{ci}\tau_i$) is determined using measured plasmas parameters, where ω_{ci} and τ_i and ion gyro-frequency and collision time respectively. Temporal dynamics of the computed radial electrical field, driven by the measured charge flux, are shown in Fig. 6. The radial electric field is slowly increasing prior to a sawthooth crash due to a small magnetic fluctuation-induced charge flux during this time. A maximum is reached after a surge of charge flux at the sawtooth crash. Since the charge flux diminishes immediately after the crash, the radial electric field is dissipated by classical viscous damping. The electric field relaxation time is sensitive to impurities which increase at the crash and we use Z_{eff}=6 in our modeling.

The saturated radial field spatial profile is plotted in Fig.7, where the radial field is seen to have a profile similar to the charge flux (see Fig.4), changing the sign across the resonant surface. The maximum radial electric field can reach 1~2 kV/m. Induced radial electric field points toward the resonant surface on either side, indicating a local potential well is created. Confirmation of this implied drop in potential during the sawtooth crash comes from Heavy Ion Beam Probe (HIPB) measurements in MST where a ~1 kV decrease is observed [25]. However, details of the potential structure are not known. The locally strong electric field can

be associated with spontaneous $E \times B$ driven flow which is a toroidally and poloidally symmetric (m=0, n=0) zonal flow structure with finite $k_r \approx 2\pi/w = 1.2 \; cm^{-1}$, where w is electric field spatial extent. This flow changes sign across the tearing mode resonant surface thereby imparting no net momentum. The tearing mode driven zonal flow is comparable to the measured 10 km/s mean perpendicular flow. Magnetic fluctuation-induced charge flux is strongly associated with the Maxwell stress $< \delta\vec{B}\delta\vec{B} >$. Ion flow measurements [26] are presently ongoing at MST to spatially resolve the zonal flow structure implied by the measured charge transport. An important result here is that even small magnetic fluctuation-induced charge flux is sufficient to generate a large zonal flow structure.
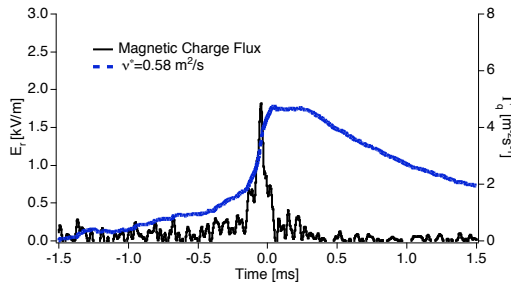

Fig. 6. Radial electric field dynamics and charge flux over a sawtooth cycle. t<0 corresponds to times before the sawtooth crash.
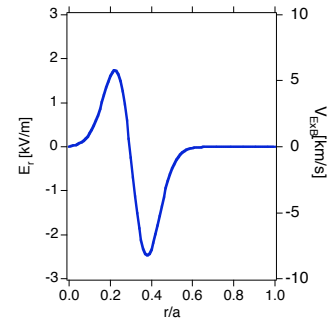

Fig. 7. Radial electric field profile and ExB flow profile after sawtooth crash (t=0.25 ms). The variation of B with minor radius is ignored here .

4. Summary

Magnetic fluctuation-induced particle transport generating non-zero charge flux driven by a global resistive tearing mode has been experimentally measured in the core of a high-temperature plasma. The charge flux dominates in the vicinity of the tearing mode resonant surface and reverses the sign across the resonant surface. Three wave coupling, altering the phase relation between the current density and magnetic field fluctuations, results in significant Maxwell stresses and charge flux at sawtooth-induced reconnection events. Modeling indicates the measured charge flux, including shielding from the ion polarization drift, can result in the buildup of a significant radial electric field and electric field shear. Relaxation occurs on a classical viscous time scale. The flow pattern associated with the fluctuation-induced radial electric field reveals an m=n=0 zonal flow structure.

References:

[1] K.Itoh, S.-I. Ithoh, P.H. Diamond, T.S. Hahm, A. Fujisawa, G.R. Tynan, M. Yagi and Y. Nagashima, Physics of Plasmas, **13**, 05502 (2006).
[2] C.J. McDevitt and P.H. Diamond, Physics of Plasmas, **13,**032302(2006).
[3] A. B. Rechester and M. N. Rosenbluth, Phys. Rev. Letts. **40**, 38(1978).
[4] J. D. Callen, Phys. Rev. Letts. **39**, 1540(1977).
[5] J.Wesson, *Tokamaks* (Oxford University Press, New York, 1997).
 [6] P.C. Liewer, Nucl. Fusion, **25,** 543(1985).
[7] M.R. Stoneking, S.A. Hokin, S.C.Prager, G.Fiksel, H. Ji and D.J. Den Hartog, Phys. Rev. Letts. **73,**549(1994).
[8] T.D. Rempel, *et al.* Phys. Fluids B **4**, 2136(1992).
[9] W. Shen, R.N.Dexter, and S.C. Prager, Phys. Rev. Letts. **68,**1319(1992).
[10] Neal A. Crocker, Ph.D dissertation, University of Wisconsin, Madison (2001).
[11] T.E. Stringer, Nuclear Fusion, **32,**1421(1992).
[12] R.E.Waltz, Phys. Fluids, **25,**1269(1982).
[13] R.N. Dexter, D.W.Kerst, T.W.Lovell, S.C. Prager, and J.C. Sprott, Fusion Technol. **19,**131(1991).
[14] H.A.B. Bodin, Nuclear Fusion, **30,**1717(1990).
[15] W.X. Ding, D.L. Brower, B.H. Deng, D. Craig, S.C. Prager, V. Svidzinski,Rev. Sci. Instrum. **75,** 3387(2004).
[16] W. X. Ding, D. L. Brower, S. D. Terry, D. Craig, S. C. Prager, J. S. Sarff, J. Wright, Phys. Rev. Lett. **90,** 035002(2003). W. X. Ding, *et al.* Phys. Rev. Lett. **90**, 035002(2003).
[17] N. E. Lanier, *et al.* Physics of Plasmas, **8**, 3402 (2001).
[18] S.D. Terry, D.L. Brower, W.X. Ding, J.K. Anderson , T.M. Biewer , B.E. Chapman , D.Craig , C.B. Forest , S.C. Prager , J.S. Sarff, Phys. Plasmas **11**, 1079(2004).
[19] R.Fitzpatrick, Nuclear Fusion **33**, 1049(1993).
[20] A.K. Hansen, A.F.Almagri, D. Craig, D.J.Den Hartog, C.C. Hegna, S.C. Prager and J.S. Sarff, Phys. Rev. Lett. **85**,3408(2000); S.Assadi, S.C. Stewart, and K.L.Sidikman, Phys. Rev. Letts. **69**, 281(1992).
[21] R.G. Watt and R.A. Nebel, Phys. Fluids **26**, 1168(1983).
[22] T. Bolzonella, D. Terranova, Plasma Physics and Controlled Fusion, **44**, 2569(2002).
[23] S.Inoue, T. Tange, K. Itoh, and T. Tuda, Nuclear Fusion **19**.1252(1979).
[24] K.Itoh and S.Itoh, Plasma Physics and Control Fusion **38,** 1(1996)
[25] J. Lei, *et al* . Phys. Rev. Letts. **89**,275001(2002).
[26] D. Craig , D. Den Hartog, G. Fiksel , V.I. Davydenko, A.A. Ivanov, Rev. Sci. Instrum. **72**, 1008(2001).